JOURNAL OF MATERIALS SCIENCE 31 (1996) 5231–5238

Interfacial mobility and its effect on interlaminar fracture toughness in glass-fibre-reinforced epoxy laminates

T. W. H. WANG, F. D. BLUM*
Department of Chemistry and Materials Research Center, University of Missouri-Rolla, Rolla, MO 65409, USA

The effects of interfacial treatment of glass fibres in glass/epoxy composites were studied through Mode I delamination fracture toughness tests using a double cantilever beam specimen. The treatment of glass fibres with two similar silane coupling agents has been shown to improve the mechanical properties of the composite as a function of the type of coupling agent. γ-aminopropyltriethoxysilane (APS) and γ-aminobutyltriethoxysilane (ABS) have similar chemistry, but differ in mobility (molecular motion) at the coupling agent–epoxy interface. The critical energy release rate, G_{1c}, for the APS-treated composites (0.59 ± 0.05 kJ m^{-2}) was shown to be higher than that of the ABS-treated one (0.37 ± 0.01 kJ m^{-2}) and also the untreated one (0.31 ± 0.02 kJ m^{-2}). In this case, the bulk structural property appears to be a function of the microscopic interfacial properties including the dynamics of the coupling agent layer. Optical characterization of the fracture surfaces reveal delamination at the epoxy–glass interface for the untreated samples, while the ABS- and APS-treated samples showed less interfacial delamination, respectively.

1. Introduction

Laminates based on glass fabrics are used in a variety of structural applications for reinforcement. Fibre-reinforced polymer composites (FRP) often consist of two major components: an inorganic phase, such as glass fibres, and an organic polymer matrix, such as an epoxy resin. The function of the polymer matrix is to bind the fibres together, transfer the load to them, and to protect them from environmental effects [1].

The physical properties of composite materials are determined by the properties of their components and composite structure. In addition, properties of the interfacial region significantly contribute to the bulk properties. It is difficult to separate the contribution of each to the composite behaviour. This is particularly true with the organic polymer phase because its molecular level behaviour can be influenced by chemical or physical interactions at the inorganic particle interface. The interfacial material between the matrix and fibre has effectively to transfer the load from the polymer to the reinforcing fibres. A weak interface may result in the failure of the composite. Strong interfacial interactions may be achieved through chemical bonding. This has been shown to be important for transverse strength and resistance to environmental factors [2, 3].

The microscopic nature of the interface often makes it difficult to study with conventional techniques. Microscopic probes of interfacial properties can conveniently be classified as relating to either structure or dynamics. A structural property, for example, might be the conformation of a molecular on a solid surface or the mechanism by which it was attached to it. A dynamic or motional property might be the rate and manner in which the molecule moves when attached to the surface. These two are clearly interrelated, but different, and different experimental techniques are usually sensitive to different kinds of properties.

One way to achieve better interfacial properties in composites is through the use of coupling agents. Silane coupling agents are widely used as finishing agents for glass fabrics [2, 4]. They are used to improve the adhesion between the two constituents in a polymer composite and can act as a bridge between the glass fibre and the matrix. The presence of a small amount of coupling agent in the composite can greatly enhance its properties. This is particularly important in the presence of moisture, which is responsible for many composite failures [2].

Aminosilanes are among the most used coupling agents. A significant amount of work, based on various techniques, has been done to elucidate the structure of aminosilanes in solution and on substrates [5–11]. The majority of these studies has focused on the structure of the coupling agents at or near the surface. In addition to structure, knowledge of the

---

*Author to whom all correspondence should be addressed.

0022–2461

molecular motion of the coupling agents may provide a better understanding of their behaviour and relationship to the physical properties of composites. Because molecular motion may vary from system to system, some consideration of the interface mobility is appropriate in the understanding of the composite properties.

The focus of the present work was to determine if the mobility of the coupling agents plays a role in the physical properties of composites. To do this we chose to compare the physical properties of composites with two coupling agents (aminosilanes) of different mobility. Epoxy resins were chosen in this study because of the technological importance and also (i) they adhere well to a wide variety of fillers and fibres, (ii) a wide variety of epoxy resins and curing agents can be formulated to give a broad range of properties, (iii) the epoxy reaction does not release any volatile compounds, and (iv) they are chemically resistant and provide good electrical insulation [12].

The correlation between mobility and physical properties was mainly determined through the use of interlaminar fracture toughness tests. In structural materials, a major concern is resistance to delamination, and toughness in this mode is frequently assessed using a double cantilever beam (DCB) specimen. DCB specimens have previously been used [13, 14] to characterize mode I delamination fracture toughness. The interlaminar fracture toughness of the treated glass composites was measured and compared with that of untreated composites. In addition, optical characterization was employed using a microscope in order to examine the delamination of the resin and fibres. These established the relationship between the interfacial mobilities and the physical properties of the fibre/resin composites.

2. Experimental procedure

The E-glass fibre fabric used was made and donated by the Owens-Corning Fiberglas Co. (Granville, OH). The glass fabrics used (ECG 7628) were plain weaved from stranded E-glass filaments (ECG 150 4/2 3.8S) [15]. The strands consisted of two four-ply filaments whose primary fibre was continuous with a 13 μm nominal diameter. γ-aminopropyltriethoxysilane (APS) was purchased from Hüls America (Piscatway, NJ) and used as-received. γ-aminobutyltriethoxysilane (ABS) was prepared by hydrogenation of cyanopropyltriethoxysilane (CPS, Hüls America) under a pressure of 100 p.s.i (10^3 p.s.i = 6.89 N mm^{-2}) in the presence of Raney nickel catalyst [16, 17]. The product was then vacuum distilled at 30 mm Hg and 85 °C. It was analysed by Fourier transform–infrared spectroscopy (FT-IR) ^{13}C and ^{1}H nuclear magnetic resonance (NMR). A yield about 50% was typically obtained [17, 18].

The epoxy resin, diglycidylether of bisphenol A (DGEBA), labelled DER 331, was obtained from the Dow Chemical (Midland, MI) and used as-received. The measured epoxy equivalent weight (EEW) was 163 g eq^{-1} according to established procedures [19, 20]. The hardener for curing the epoxy, diethylenetriamine (DETA), was also obtained from Dow (DEH20) and also used as-received. For thorough cross-linking, a 1:1 stoichiometric ratio between available hydrogen from amines and epoxy groups was used. This corresponded to an epoxy/hardener ratio of 10:1 by weight.

The deposition of silane coupling agents on to the glass fabrics was conducted in a manner based on that of Blum *et al.* [16]. A 2% solution of the coupling agent was hydrolysed in acetone/distilled water (10/1) for 24 h. The heat-cleaned glass fabrics which were cut into 15.24 × 15.24 cm^2 pieces were then immersed into the solution for 24 h at room temperature. The treated glass fabrics were washed several times with distilled water and then dried in a vacuum oven at 110 °C for 0.5 h. The amount of silane coupling agent deposited on the surface of the glass fabrics was determined by gravimetric analysis following heat treatment in an oven at 600 °C for 12 h. The amount of coupling agents deposited was estimated to be 0.35 wt% of the bare glass fabric. Based on a knowledge of the monolayer coverage of about 4 silanols/1.00 nm^2 [16], this corresponded to between 30 and 290 layers, depending on the model used to estimate the effective surface area of the glass. For example, if the area is calculated, assuming the glass was simply a plane sheet, a maximum of about 290 layers is estimated. If the woven filaments were laid out so that they were touching side by side, about 90 layers would result. If all of the surface of every primary fibre was available to accept coupling agents, an estimated 30 layers would result. Clearly, the number of layers is likely to be between the two extremes and, in any case, represents multilayer behaviour.

The epoxy/hardener (10:1) was well stirred for several minutes, laminates were obtained by hand lay-up with 16 treated or untreated glass-fabric layers in a 15.24 cm × 15.24 cm aluminum mould, and cured in a hot press at 115 °C for 30 min with a pressure about 6.9 MN m^{-2}. To ensure complete chemical reaction, the laminates were further postcured at 140 °C for 1 h DSC traces were consistent with complete epoxy reaction under these conditions. The laminates were then cooled slowly overnight to reduce residual stresses.

The size and geometry of our DCB specimens is shown in Fig. 1. A sharp starter crack was introduced by inserting a sheet of aluminium foil (0.7 μm) between the centre laminate of the composite. The specimens were loaded at a crosshead speed of 0.2 cm min^{-1} using an Instron model 4204 through the copper hinge glued to the specimen.

The fracture toughness of the specimen was estimated from the critical strain energy release rate. In principle, when a crack propagates in an elastic body under external load, a constant energy is released to form the new surface. This energy per unit area is called the strain energy release rate. At the point of crack initiation or arrest, this value is known as the critical strain energy release rate (or fracture toughness), G_{1c} [21] which is given by

$$G_{1c} = (P_c^2/2B)(\partial C/\partial a) \qquad (1)$$

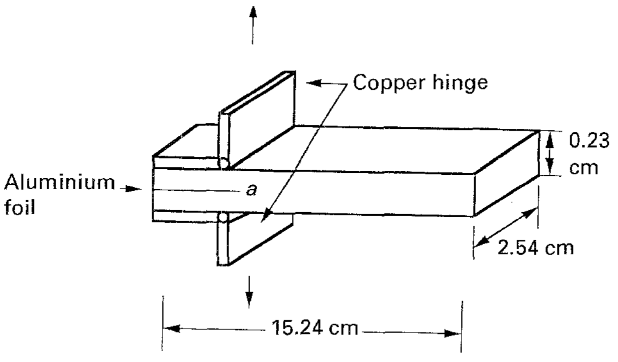

Figure 1 Geometry of the double cantilever beam (DCB) specimen. (The crosshead speed was 0.2 cm min^{-1} and the initial crack length was 3.81 cm.)

where P_c is the applied load at crack initiation or reinitiation, B the specimen width, C the compliance and a the crack length. From the load–displacement curves, the compliance, C, is obtained and when plotted against a, $\partial C/\partial a$ is obtained. The C–a relationship has been approximated by [22]

$$C(a) = Ra^n \tag{2}$$

where R and n are constants which are experimentally determined. From Equations 1 and 2, the critical strain energy release rate is given by [22]

$$G_{Ic} = nP_c^2C(a)/(2Ba) \tag{3}$$

3. Results

3.1. Load–displacement curve and fracture toughness

The load–displacement curves obtained can be divided into two categories based on their crack propagation behaviour. The first is a stable crack propagation growth pattern and is shown for representative runs in Fig. 2. This was usually the case. The curves are displaced along the load axis for clarity. For these, the cracks grew slowly during propagation. The second is unstable crack growth. In this case, the test was stopped at the point where the crack was arrested. The new crack tip was then marked and the machine reset to zero load. The load was applied again and the crack propagated. This procedure was repeated as often as necessary.

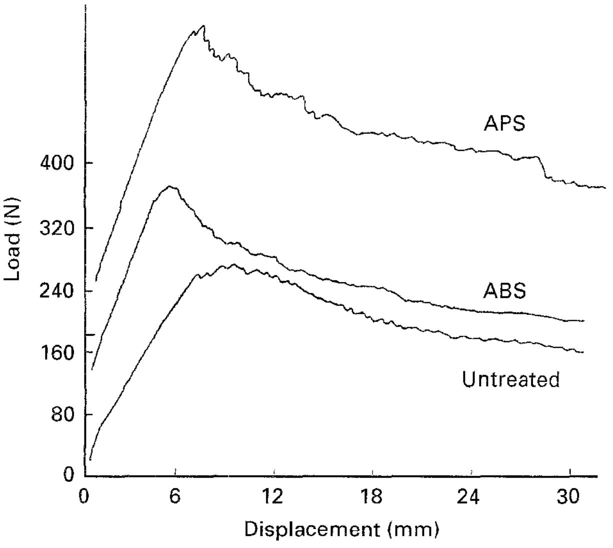

Figure 2 Typical load–displacement curves for untreated, ABS-, and APS-treated glass fibre-reinforced epoxy composites.

The compliance, C, was calculated from the load–displacement curves and plotted against the crack length. Fig. 3a shows typical C–a curves on double logarithmic plots based on point of crack initiation. These relationships can be approximated by Equation 2. The values of n were equal to 3.45 for

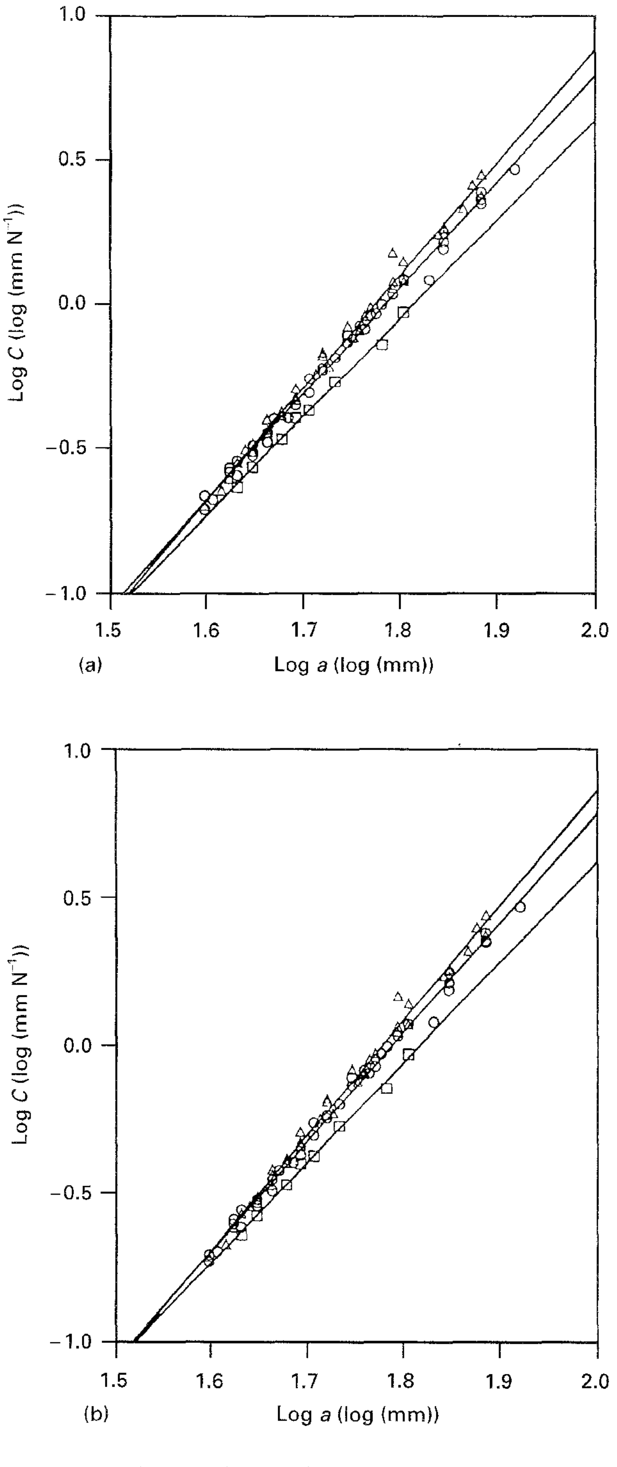

Figure 3 Double logarithmic plot of typical compliance–crack length (c–a) relationships based on point of (a) crack initiation, and (b) crack arrest for (□) untreated, (○) ABS- and (△) APS- treated samples.

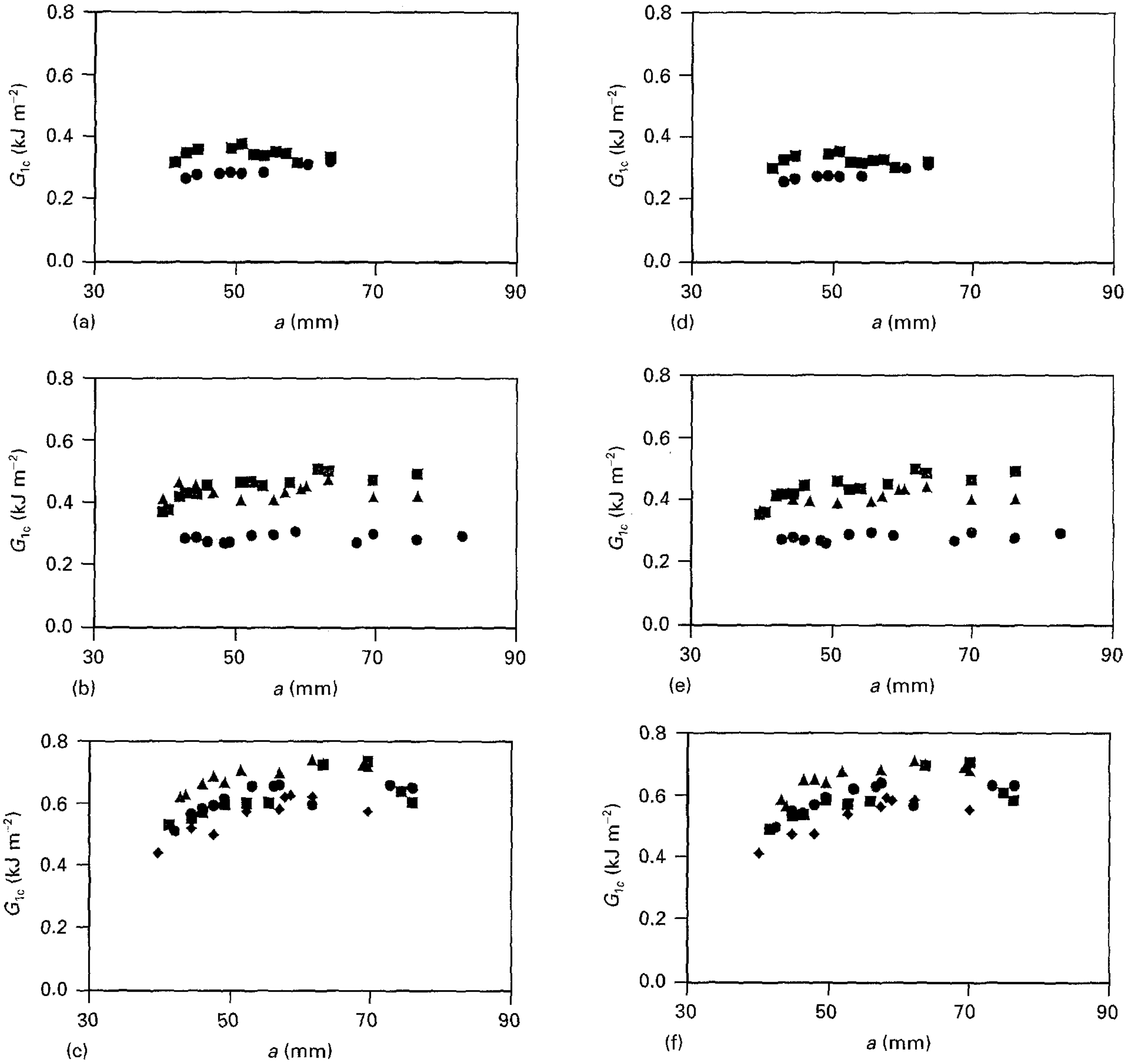

Figure 4 Critical energy release rate, G_{1c}, of the (a, d) untreated, (b, e) ABS- and (c, f) APS-treated composites (from top to bottom, respectively) as a function of crack length based on point of (a-c) crack initiation and (d-f) crack arrest. The different symbols represent different runs.

untreated glass composites, 3.78 for ABS-treated composites, and 3.97 for APS-treated composites.

The *C–a* curves for crack arrest are shown in Fig. 3b. The value of *n* was equal to 3.44 for untreated composites, 3.70 for ABS-treated composites, and 3.92 for APS-treated composites. For both crack initiation and arrest, the values of *n* increased from untreated < ABS < APS treated composites. The actual values of *n* were also very similar from either crack initiation or arrest. Using the calculated *n* values in Equation 3, the critical strain energy release rate is calculated.

The critical strain energy release rate based on the point of crack initiation for the three types of composites as a function of the crack length are shown in Fig. 4a–c. Fig. 4d–f shows those values calculated based on the point of crack arrest. The values of G_{1c} of the untreated composites were approximately independent of the crack length (Fig. 4). In contrast, the values of G_{1c} for ABS- and APS-treated composites are more dependent on the crack length. In the range of small crack lengths, the G_{1c}s of the ABS-treated composites are almost equal to those of the untreated composites. When the crack length was above 50 mm, higher G_{1c} values were obtained for ABS-treated composites. Increased G_{1c}s were also found in APS-treated composites with increasing crack length. The value for APS-treated material was the highest measured for all three samples.

The values of G_{1c} for the untreated glass composites calculated at point of arrest was approximately independent of crack length. The G_{1c} value of the ABS-treated composite was intermediate between the untreated and APS-treated composites. G_{1c} values for APS-treated composite calculated at point of arrest were shown to increase with crack length. The averaged G_{1c} values obtained at the point of crack initiation (or reinitiation) and arrest are shown in Table I together with the measured *n* values.

3.2. Macroscopic observations

Photographs of the fracture surface of the three different specimens are shown in Fig. 5a–c. The untreated-glass sample has one side covered with epoxy resin

TABLE I The slopes of compliance–crack growth plots, n, and average critical energy release rate, G_{Ic}, based on crack initiation (superscript i) and crack arrest (superscript a)

	n^i	n^a	G^i_{Ic} (kJ m^{-2})	G^a_{Ic} (kJ m^{-2})
Bulk	3.45	3.44	0.32 ± 0.03	0.31 ± 0.02
ABS	3.78	3.70	0.39 ± 0.11	0.37 ± 0.10
APS	3.97	3.92	0.61 ± 0.05	0.59 ± 0.05

and the other (mating surface) (Fig. 5a) reveals bare glass-fibre fabric. Thus the crack propagated neatly along the glass/epoxy interface. The ABS-treated materials, Fig. 5b, show surfaces where there are patches from the crack propagating along the glass/epoxy interface. For the APS-treated specimen of Fig. 5c, the patches of interfacial failure are smaller and there are several ribbon-like sections running along the length of the specimen. The ABS-treated specimen has fewer ribbons than the APS-treated specimen and is more closely related to the untreated specimen which has mainly epoxy on one surface and bare glass on the other.

Optical micrographs of the fracture surfaces for the DCB specimens are shown in Fig. 6a–c. Fig. 6a shows the stable crack growth of untreated specimen with exposed glass-fibre fabric without epoxy resin. The matted surface is covered with unbroken epoxy resin. The ABS-treated specimen in Figure 6b shows that its crack growth resulted in some broken resin patches. Its fracture surface is covered with less resin than the APS-treated specimen. Fig. 6c shows the stable crack growth of APS-treated specimen, the fracture surface is mainly covered with resin on both sides. This means that the stable crack growth of the APS-treated specimen propagates mainly through the epoxy and that of the untreated specimen propagated through the interface. ABS treatment resulted in intermediate behaviour.

4. Discussion

Numerous studies have focused on the interfacial mechanical properties, especially interlaminar fracture of composites. Suzuki *et al.* [13] investigated the influence of silane coupling agents on interlaminar fracture in glass-fibre fabric-reinforced unsaturated polyester laminates. They found that the fracture toughness and the crack propagation behaviour were dependent on the types (methacryl- versus epoxy-silane) and concentration of silane coupling agents used. The critical energy release rates found were about 0.4 kJ m^{-2} for stable cracks, and between 0.2 and 0.6 kJ m^{-2} for unstable cracks. It was also suggested that an optimum silane amount on the glass fibre should be achieved in order to increase the delamination resistance of the composites. Bazhenov [14] studied the effect of strong bending in the DCB interlaminar test of thin, E-glass woven fabric-reinforced epoxy laminates. The interlaminar fracture toughness (1.05–1.25 kJ m^{-2}) of the fabric-reinforced laminates was significantly higher, by 5–10 times, than those of non-woven unidirectional composites. This was believed to be because the plastic yield zone was restricted by the space between the fabric layers, which was much larger than that between adjacent fibres in the unidirectional layer. Without the fibre sizing agent, the interlaminar fracture toughness, G_{Ic}, was reduced to 0.77 kJ m^{-2}. It was further reduced to 0.2 kJ m^{-2} after exposure in water.

The effect of silanes on the interfacial properties of fibrous composites were studied by Chua *et al.* [23]. These workers mixed monomeric coupling agents with the resin and carried out single-fibre pull-out

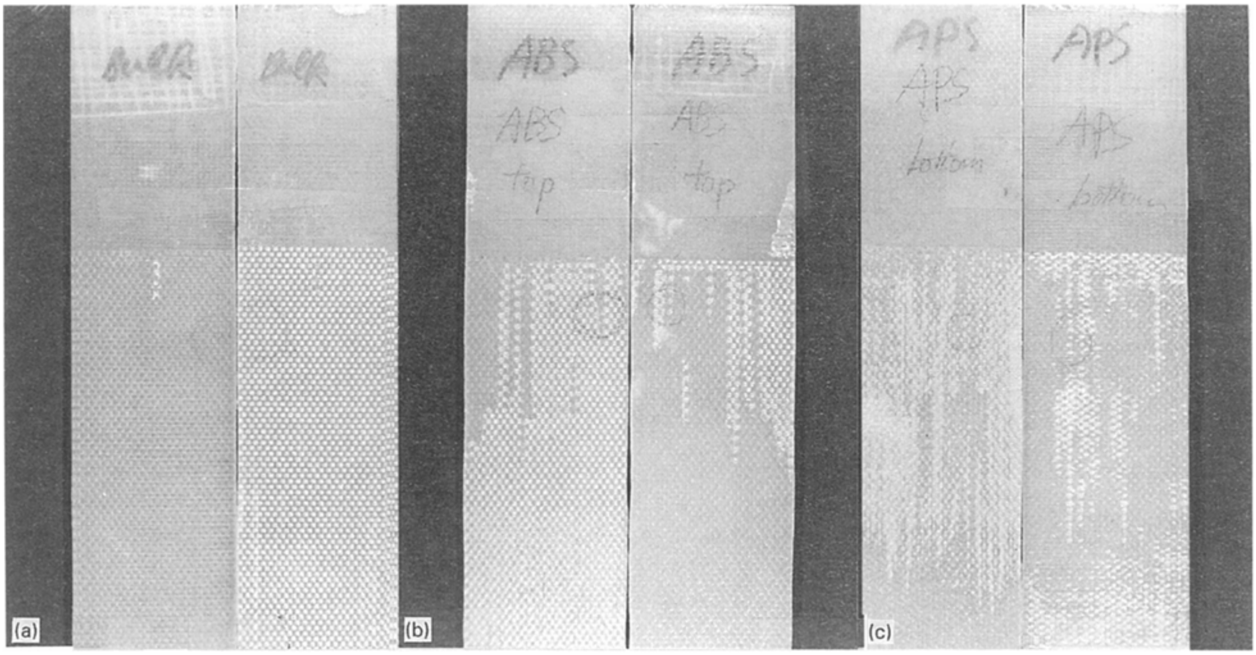

Figure 5 Macroscopic observations of the fracture surface of (a) untreated composites, (b) ABS-treated composites, and (c) APS-treated composites.

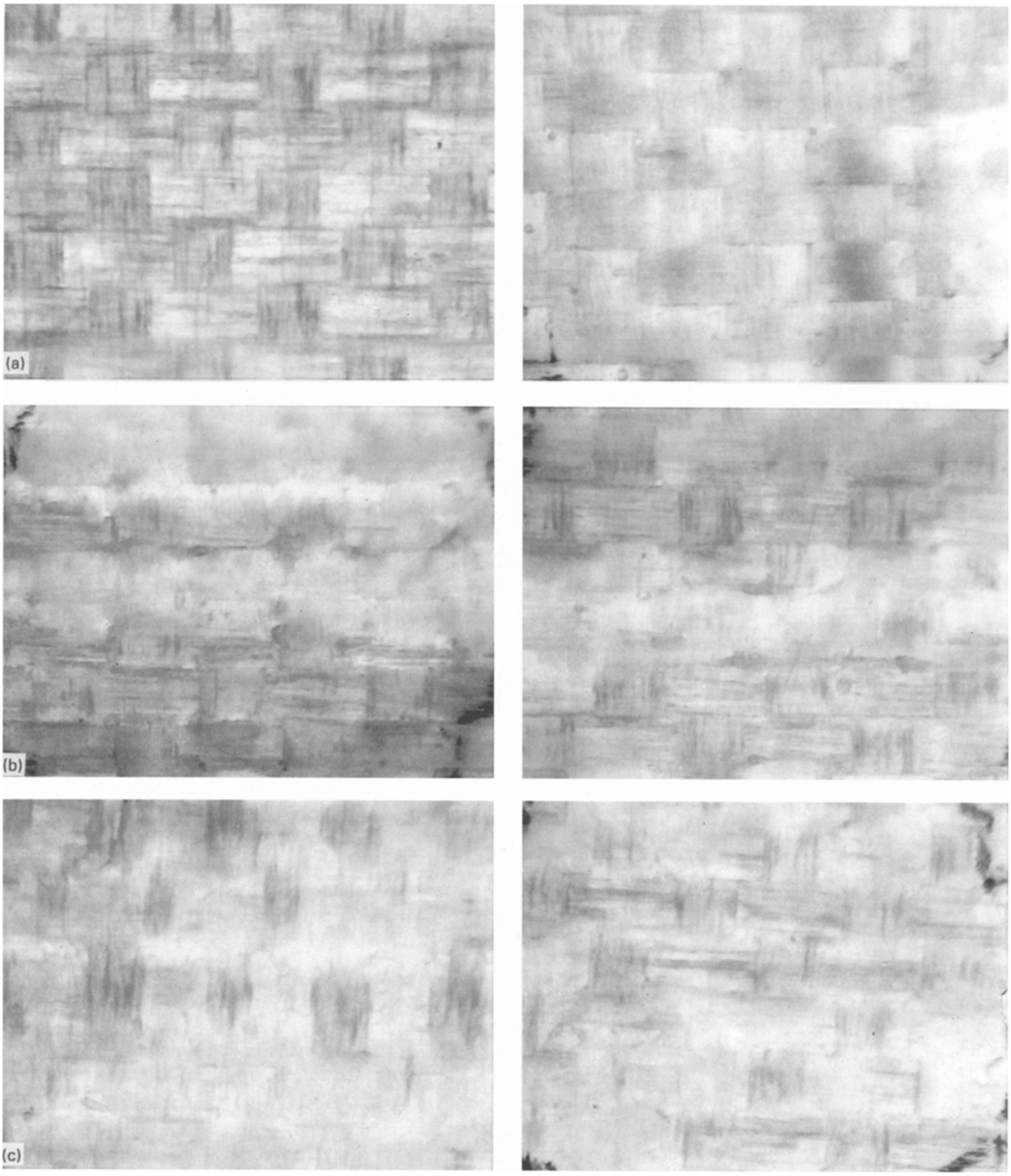

Figure 6 Optical microscopic observations (X4) of the fracture surface of (a) untreated composites, (b) ABS-treated composites, and (c) APS-treated composites.

tests. Removal of the commercial coating on the fibres successively increased the bond strength between the fibre and resin. Mixing of the coupling agent with the resin did not improve the physical properties of the composite because it caused the plasticization of the resin. This suggests that direct fibre treatment with the coupling agent is probably preferred. The influence of the thickness of the silane coupling agent on the interfacial properties of fibrous composites was studied by Yue and Quek [24] using the single-fibre pull-out test. They indicated that maximum interfacial shear strength was obtained at a critical thickness of the silane layer on the treated fibre. Both the interfacial frictional stress and the interfacial coefficient of friction decreased with increased thickness of the silane coating.

Of particular interest to us is the role that molecular motion of the interfacial material plays in the composites. It is well established that molecular motions determine many of the physical properties of polymers [25]. Nuclear magnetic resonance (NMR) studies provide a useful way of determining these. Some studies have correlated macroscopic properties of polymers with dynamics via NMR [26–30]. Liu *et al.* [26] characterized the fatigue of segmented polyurethanes and found that the segmental motion at the interfaces around the hard domains decreased the intensity of the ^{13}C NMR resonance in the early stages of fatigue. At longer fatigue cycles, the resonance disappeared. Parker *et al.* [27] established a relationship between dynamic storage modulus and CPMAS–NMR cross-polarization rates.

NMR has also been used to probe the mobility interfacial species in composites [31]. Previous work from our laboratory [32, 33] has used ^{29}Si CP/MAS to verify bonding of aminopropyltriethoxysilane and aminobutyltriethoxysilane coupling agents to silica. ^{2}H wide-line NMR was also used to yield information on the nature of the structure and dynamics of the selectively deuterated aminofunctional silanes adsorbed on silica surfaces as a function of composition. Semi-detailed information on the motional rate and the types of motion have been obtained from a comparison of the experimental and simulated deuterium line shapes [16, 33–36]. The results from ^{2}H NMR spectra for deuterated-APS (DAPS) and deuterated-ABS (DABS) on silica [16, 32] showed that the difference in the alkyl chain length of the coupling agents results in different motional rates. For the first coupling agent layer (monolayer), ABS and APS have similar mobilities. However, ABS moves about ten times faster than APS at the "outer" layers of coupling agent. We believe that this difference plays a role in the measured fracture toughness.

In the present work, the presence of either coupling agent increased the fracture toughness of the composite. This is due, at least in part, to the chemical bonding which occurs at the interface. The lower G_{Ic} value for the ABS-treated composite suggests poorer interfacial properties which appear to transfer the load less effectively from the resin to the fibres. Thus, APS imparts better properties than ABS in these composites. Because the chemistry of APS and ABS is similar, almost identical, the differences are probably due to the dynamics. To the best of our knowledge, no one has established a relationship between the molecular motion of the interface and bulk mechanical properties of composites. Our results suggest that, in addition to the chemical properties of interfacial species such as coupling agents, dynamical properties should also be considered.

We wish to speculate on *why* differences in the dynamics of the interfacial layers produce differences in physical properties. The relationship between molecular motion and modulus is well established [25]. Previous work from our group has shown that a motional gradient is formed when coupling agents are adsorbed on the silica [16, 32]. This suggests that there is also a gradient in the physical properties (modulus) in the interfacial layer. Considering that there is a mismatch in properties (e.g. modulus) between the glass fibre and epoxy resin, the presence of an interfacial layer with a motional gradient would be expected to allow a smoother transition from the properties of one material to another. Both ABS and APS have similar mobilities at the glass-coupling agent interface. The first layer of coupling agent is relatively rigid, however, on the other side of the coupling agent layer, the ABS system has significantly more mobility than that of APS. We propose that APS has better matching of properties at the APS–epoxy interface resulting in better physical properties. The ABS system is too mobile (i.e. too flexible) at this interface. We believe that this is why APS has been so successful as an adhesion promoter for glass/epoxy applications instead of the other alkyl species which, in principle, could be made equally inexpensively in large quantities.

5. Conclusions

A fracture toughness test, using a DCB specimen, has been used to probe how coupling agents with different mobilities affect the physical properties of glass fabric laminates. Interlaminate fracture toughness of glass-fibre fabric epoxy composites is influenced by the type of silane coupling agent used. Untreated composites have the lowest critical energy release rate resulting from a poor interface between fibre fabrics and resin. Poor interfacial properties resulted in a delamination between the resin and fibres. ABS-treated composites show improvement due to the presence of the coupling agents. They have a higher critical energy release rate than the untreated composites. The APS-treated composites have the highest critical energy release rates. We believe that this is probably due to the shorter alkyl chain lengths and lower mobility of the APS layers. This coupling agent provides a better graded interface than ABS. Consideration of the mobility of the coupling agent layer should allow the most effective choice of an appropriate interfacial system for coupling agent applications.

Acknowledgements

We gratefully acknowledge helpful discussions with Professor L. R. Dharani and Mr. P. Gopal and the financial assistance of the Office of Naval Research. We also thank Mr Robert J. Sauer, Owens-Corning Fiberglas Co., for supplying us with heat-treated fabric.

References

1. B. D. AGARWAL and L. J. BROUTMAN, "Analysis and Performance of Fiber Composites", 2nd Edn (Wiley, New York, 1990).
2. E. P. PLUEDDEMANN "Silane Coupling Agents", 2nd Edn (Plenum Press, New York, 1991).
3. R. HOLTMAN, *Kunststoffe* **55** (1965) 903.
4. C. E. KNOX, in "Handbook of Composites", edited by G. Lubin (Van Nostrand Reinhold, New York, 1982) Ch. 4.
5. C. H. CHIANG, H. ISHIDA and J. L . KOENIG, *J. Coll. Interface Sci.* **74** (1980) 396.
6. M. E. SCHRADER, *J. Adhesion* **2** (1970) 202.
7. S. R. CULLER, H. ISHIDA and J. L. KOENIG, *J. Coll. Interface Sci.* **06** (1985) 334.
8. H. ISHIDA, *Polym. Compos.* **5** (1984) 101.
9. G. E. MACIEL and D. W. SINDORF, *J. Am. Chem. Soc.* **102** (1980) 7606.
10. D. E. LEYDEN, D. S. KENDALL and T. G. WADDELL, *Anal. Chim. Acta* **125** (1981) 207.
11. A. M. ZAPER and J. L. KOENIG, *Polym. Compos.* **6** (1985) 156.
12. L. S. PENN and T. T. CHIAO, in "Handbook of Composites", edited by G. Lubin (Van Nostrand Reinhold, New York, 1982) Ch. 5.

13. Y. SUZUKI, Z. MAEKAWA, H. HAMADA, A. YOKOYAMA and T. SUGIHARA, *J. Mater. Sci.* **28** (1993) 1725.
14. S. L. BAZHENOV, *Composites* **22** (1991) 275.
15. "Textile Fibers for Industry", Owens/Corning Fiberglas Co. (1985), publication 5-TOD8285-C.
16. F. D. BLUM, W. MEESIRI, H. J. KANG and J. E. GAMBOGI, *J. Adhes. Sci. Technol.* **5** (1991) 479.
17. J. STEIN, S. J. VALENTY, D. V. BREZNIAK and L. C. PRUTZMAN, *Macromolecules* **19** (1986) 2291.
18. H. J. KANG, W. MEESIRI and F. D. BLUM, *Mater. Sci. Eng.* **A126** (1990) 265.
19. J. G. DORSEY, G. RUTENBERY and L GREEN, *Anal. Chem.* **49** (1977) 1144.
20. A. HAMMERICH and F. G. WILLEBORDSE, *ibid.* **45** (1973) 1696.
21. H. L. EWALDS and R. J. H. WANHILL, "Fracture Mechanics" (Edwald Arnold, London, 1984).
22. J. P. BERRY, *J. Appl. Phys.* **34** (1963) 62.
23. P. S. CHUA, S. R. DAI and M. R. PIGGOTT, *J. Mater. Sci.* **27** (1992) 913.
24. C. Y. YUE and M. Y. QUEK, *ibid.* **29** (1994) 2487.
25. J. D. FERRY, "Viscoelastic Properties of Polymers", 3rd Edn (Wiley, New York, 1980).
26. L. B. LIU, M. SUMITA and K. J. MIYASAKA, *J. Macromol. Sci. Phys.* **B28** (1989) 309.
27. A. A. PARKER, J. J. MARCINKO, Y. T. SHIEH, D. P. HEDRICK and W. M. RITCHEY, *J. Appl. Polym. Sci.* **40** (1990) 1717.
28. A. P. LEGRAND, N. LECOMTE, A. VIDAL, B. HAIDAR and E. PAPIRER, *ibid.* **46** (1992) 2223.
29. T. P. HUIJGEN, H. ANGAD GAUR, T. L. WEEDING, L. W. JENNESKENS, H. E. C. SCHUURS, W. G. B. HUYSMANS and W. S. VEEMAN, *Macromolecules* **23** (1990) 3063.
30. A. A. PARKER, M. Y. TSAI, G. BIRESAW, T. T. STANZIONE, G. H. ARMSTRONG and J. J. MARCINKO, *Mater. Res. Soc. Symp. Proc.* **249** (1992) 273.
31. F. D. BLUM, in "Annual Reports of NMR Spectroscopy", Vol. 28, edited by I. Ando and G. A. Webb (Academic Press, London, 1994) p. 277.
32. H. J. KANG and F. D. BLUM, *J. Phys. Chem.* **95** (1991) 9391.
33. J. E. GAMBOGI and F. D. BLUM, *Macromolecules* **25** (1992) 4526.
34. J. H. FREED, in "Spin Labelling: Theory and Applications", Vol. 1, edited by L. Berliner (Academic Press, New York, 1976) 53.
35. D. J. SCHNEIDER and J. H. FREED, in "Spin Labelling", Vol. 8, edited by L. Berliner (Academic Press, New York, 1989) p. 1.
36. S. JAGANNATHAN, F. D. BLUM and C. F. POLNASZEK, *J. Chem. Inf. Comput. Sci.* **27** (1987) 167.

Received 14 November 1994
and accepted 16 August 1995